Nanoparticle-mediated delivery of siRNA targeting Parp1 extends survival of mice bearing tumors derived from Brca1-deficient ovarian cancer cells

Michael S. Goldberg[a,1], Deyin Xing[a,1], Yin Ren[b], Sandra Orsulic[c], Sangeeta N. Bhatia[a,b], and Phillip A. Sharp[a,d,2]

[a]David H. Koch Institute for Integrative Cancer Research, Massachusetts Institute of Technology, Cambridge, MA 02139; [b]Harvard-MIT Division of Health Sciences and Technology, Cambridge, MA 02139; [c]Women's Cancer Research Institute, Cedars-Sinai Medical Center, Los Angeles, CA 90048; and [d]Department of Biology, Massachusetts Institute of Technology, Cambridge, MA 02139

Contributed by Phillip A. Sharp, December 6, 2010 (sent for review October 4, 2010)

Inhibition of the DNA repair enzyme poly(ADP-ribose) polymerase 1 (PARP1) with small molecules has been shown to be an effective treatment for ovarian cancer with BRCA mutations. Here, we report the in vivo administration of siRNA to Parp1 in mouse models of ovarian cancer. A unique member of the lipid-like materials known as lipidoids is shown to deliver siRNA to disseminated murine ovarian carcinoma allograft tumors following intraperitoneal (i.p.) injection. siParp1 inhibits cell growth, primarily by induction of apoptosis, in Brca1-deficient cells both in vitro and in vivo. Additionally, the treatment extends the survival of mice bearing tumors derived from Brca1-deficient ovarian cancer cells but not from Brca1 wild-type cells, confirming the proposed mechanism of synthetic lethality. Because there are 17 members of the Parp family, the inherent complementarity of RNA affords a high level of specificity for therapeutically addressing Parp1 in the context of impaired homologous recombination.

drug delivery | RNAi

The overall cure rate of ovarian cancer has remained low, greatly owing to the fact that few diagnoses are made while the tumor is limited to the ovaries (1). Because the disease is so heterogeneous, enhanced outcomes await translating insights at the molecular level into personalized treatment strategies (2). Germ-line mutations of *BRCA1* confer a lifetime risk of ~85% for breast cancer and ~45% for ovarian cancer in families with multiple cases of such cancers (3). Mutations in the *BRCA1* gene occur in ~5% of ovarian cancer cases in the general population (4), and inheritance of DNA repair defects contributes to ~10% of all ovarian cancers (5). Additionally, many ovarian cancers fail to express BRCA1 due to epigenetic silencing (6). There are a number of studies showing that breast cancer tumors that assay as defective in DNA repair are also sensitive to poly(ADP-ribose) polymerase (PARP) inhibitors (7).

Cells lacking BRCA1 or BRCA2 exhibit defects in DNA repair (8). Specifically, the inability to correct double-strand breaks by homologous recombination in these mutants results in chromosomal rearrangements and genomic instability (9). PARP1 is involved in the detection of DNA damage, DNA repair, and the maintenance of genomic stability (10). Activated in response to DNA damage, PARP1 has been implicated in nonhomologous end-joining and base excision repair through both short-patch and long-patch pathways (11). It has been shown that BRCA-deficient cells exhibit profound sensitivity to inhibition of PARP1, resulting in cell cycle arrest, chromosome instability, and cell death (12, 13). In patients harboring *BRCA* mutations, an orally active PARP inhibitor has shown antitumor activity as a single agent (14). The mechanism underlying this biological outcome is known as synthetic lethality, wherein although the loss of either of two proteins alone is not lethal, the loss of both functions is catastrophic to the cell (15).

siRNA, which directs the sequence-specific degradation of target mRNA, represents a unique class of potential therapeutics for cancer (16), a disease often caused by aberrant overexpression of oncoproteins. Recently, this class of molecules was used to treat patients with melanoma upon systemic administration (17). For ovarian cancer, i.p. administration of chemotherapeutics has been shown to result in improved outcomes relative to i.v. administration (18). In view of this, we tested in a mouse model the effectiveness of delivery of nanoparticles containing siRNA targeting Parp1 for inhibition of ovarian cancer following i.p. injection.

Nanoparticles can facilitate the delivery of siRNA into cells. Previous work has demonstrated the potential of nanoparticles formed from lipid-like materials, termed lipidoids (19), in a variety of animal models, including following i.p. injection in ovarian tumor models (20). This class of materials is derived from an amine-containing backbone from which aliphatic chains extend, forming a hybrid structure that resembles dendrimers and lipids. The amines likely electrostatically interact with the phosphate backbone of siRNA and facilitate endosomal escape as the compartment becomes acidified, and the hydrophobic chains probably mediate interaction with the cell membrane.

Results

NC100 Effectively Delivers siRNA to Ovarian Cancer Cells. Cell lines and tumors with defined genetic alterations provide ideal systems in which to test the molecular mechanisms of tumor sensitivity to pathway- and/or siRNA-mediated therapy (21). We have previously developed a system in which multiple defined genetic lesions can be introduced into mouse ovarian surface epithelial cells, a cell type that is believed to be the precursor for ovarian carcinoma. This system is based on avian RCAS virus transduction of cells that are programmed to express the avian TVA receptor. Briefly, to generate ovarian surface epithelial cell lines with defined genetic alterations, we introduced coding sequences for human *c-myc*, mouse *K-ras*^{G12D}, and HA-tagged mouse myristoylated *Akt1* oncogenes into ovaries isolated from K5-TVA/p53$^{-/-}$ mice or Cre recombinase in association with oncogenes into ovaries isolated from K5-TVA/Brca1$^{lox/lox}$/p53$^{lox/lox}$ mice (21, 22). Some of the resulting cell lines generate ovarian cancer when injected into normal and immune-deficient mice.

To identify lipidoids that can be used as carriers for siRNA delivery into mouse ovarian carcinoma, 22 top-performing members of a lipidoid library were screened for the ability to transfect mT2K-Luc, a firefly luciferase-expressing murine ovarian cancer

Author contributions: M.S.G., D.X., and P.A.S. designed research; M.S.G. and D.X. performed research; Y.R., S.O., and S.N.B. contributed new reagents/analytic tools; M.S.G., D.X., and P.A.S. analyzed data; and M.S.G., D.X., and P.A.S. wrote the paper.

The authors declare no conflict of interest.

[1]M.S.G. and D.X. contributed equally to this work.

[2]To whom correspondence should be addressed. E-mail: sharppa@mit.edu.

This article contains supporting information online at www.pnas.org/lookup/suppl/doi:10.1073/pnas.1016538108/-/DCSupplemental.

cell line. The cells were treated with lipidoids complexed with 10 nM siRNA that targets this reporter (siLuc) or 10 nM siRNA that targets GFP (siGFP) to control for potential nonspecific toxicity (Fig. 1*A*). Three lipidoids—NA98, NA111, and NC100—were observed to confer robust knockdown and were selected for further evaluation, wherein a dose–response was confirmed, ranging from 1 nM to 90 nM (Fig. 1 *B* and *C*). NC100 (Fig. 1*D*) enables efficient knockdown in ovarian cancer cells in a nontoxic, dose-dependent manner and was thus selected for use in this study. Specifically, more than 90% knockdown could be observed at the mRNA level by qPCR at a dose as low as 10 nM. A related lipidoid, ND98, has been shown previously to deliver siRNA targeting the tight junction protein claudin-3 upon i.p. administration, resulting in suppression of ovarian cancer growth and metastasis (20).

NC100 was next tested for the ability to deliver siRNA to BR5FVB1, a genetically defined Brca1-deficient murine ovarian epithelial cell line that overexpresses c-myc in a $p53^{-/-}$ background (22). NC100 mediated ~65% knockdown of Parp1 mRNA after 24 h upon transfection with 5 nM siRNA (Fig. 2*A*). The extent of knockdown of Parp1 mRNA probably reflects the fraction of cells incorporating functional siParp1 into RISC, as this siRNA is highly active in other cells. This knockdown of the target gene Parp1 imparted a biological phenotype. Cells were counted 72 h posttransfection, and delivery of 20 nM siRNA targeting Parp1 was found to decrease cell numbers, slightly more so than siRNA targeting c-myc (Fig. 2*B*). FACS analysis indicated that the observed decrease in cell numbers upon transfection with siParp1 can be attributed to increased apoptosis. The percentage of apoptotic cells, which were defined as Annexin V-PE positive and 7-amino-actinomycin D (7-AAD) negative, was more than double that of cells transfected with siControl (siRNA targeting factor VII) at 48 h posttransfection with 100 nM siRNA (Fig. 2*C*). This difference was not observed at the 20-nM concentration used in the proliferation study due to a significant background of apoptosis under control conditions, making detection of an increase difficult. Indeed, even the no-treatment control exhibits a relatively high level of apoptosis in these cells, likely owing to the loss of Brca1.

A second siRNA targeting a distinct sequence within the Parp1 gene, siParp1-1, was used to confirm that the observed inhibition of cell growth was the consequence of knockdown of Parp1 and not specific to the sequence of siParp1 (Fig. S1). Consistent with the dose–response observed during screening, whereas a very robust phenotype is observed at higher siRNA concentrations in vitro, the transfection efficiency of BR5FVB1 by NC100 was observed to be only ~70% at the concentrations used for these biological assays, limiting the degree of knockdown and growth inhibition observed. Transfection efficiency was measured using dye-modified siRNA, which probably yields an overestimate of uptake, as not all siRNAs bound to cells are ultimately loaded into RISC. BR5FVB1 cells were found to be much more difficult to transfect than mT2K, the cell line in which the original screen was performed. We have observed that differential transfection efficiency across cell lines is not uncommon for lipidoid reagents, as they seem to have inherent specificity to particular cells.

Having established that NC100-mediated delivery of siParp1 yields target knockdown and inhibition of proliferation by induction of apoptosis, we confirmed that the material is well tolerated by mice upon i.p. injection (Fig. S2). Escalating doses of formulated and crudely mixed lipidoid-siRNA nanoparticles were administered to mice, and body weight was monitored at 0, 24, and 72 h. Notable weight loss was observed at the highest doses examined, but the transient decrease was not significant at 5 mg/kg, the dose used in all of the in vivo studies herein described. Next, to test whether NC100 can mediate delivery to ovarian carcinoma nodules disseminated in the i.p. cavity, Brca1 wild-type T22H cells were injected into the i.p. cavity of nude mice and allowed to grow for 2 wk. Fluorescently labeled siRNA was then formulated with NC100 and injected into the i.p. cavities of these mice at a dose of 0.5 mg/kg of labeled siRNA in 4.5 mg/kg of unlabeled siRNA. The mice were visualized 24 h later, and NC100 was found to confer greater delivery than the positive control ND98 (20) (Fig. 3*A*). Naked siRNA yielded a similar signal to the PBS negative control, confirming the importance of delivery reagents not only to protect against nucleases but also to facilitate the transport of these large, charged molecules into tissues. In

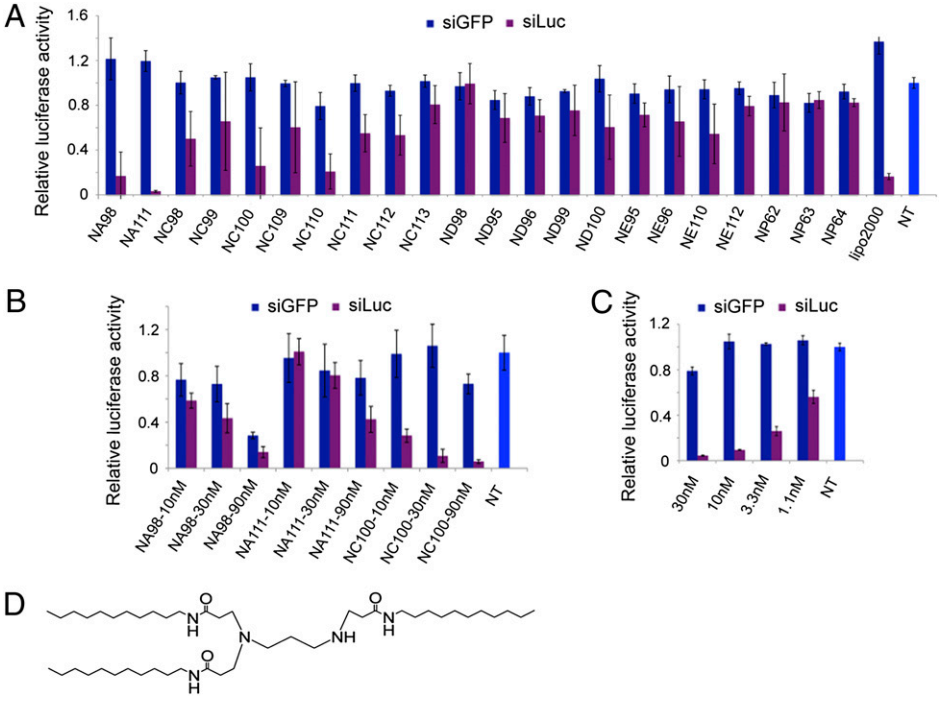

Fig. 1. The lipidoid NC100 effectively transfects ovarian cancer cell lines with siRNA. (*A*) Twenty-two top-performing members of a previously screened library of lipidoids were evaluated for the ability to knock down a luciferase reporter gene in an ovarian cancer cell line, mT2K-Luc, upon transfection with siRNA targeting luciferase. siRNA targeting GFP was used as a control. Cells were transfected with 10 nM siRNA. (*B*) The three top-performing hits from the initial screen of 22 lipidoids were reevaluated for the ability to transfect ovarian cancer cells, and NC100 was found to be the least toxic and most effective transfection reagent. (*C*) NC100 transfects ovarian cancer cells in a dose-dependent manner. (*D*) Structure of NC100. NT, no treatment. For all experiments, luciferase activity was measured after 24 h.

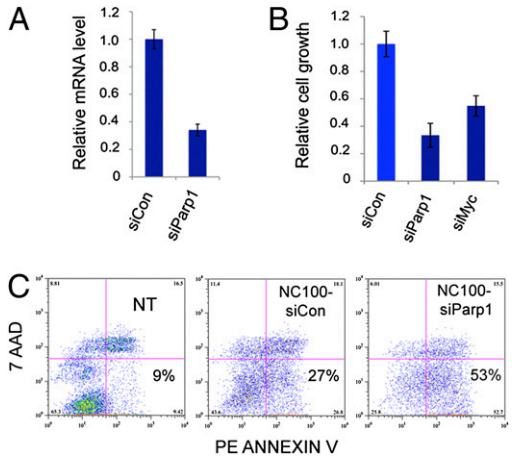

Fig. 2. Knockdown of Parp1 by NC100-delivered siRNA arrests proliferation and induces apoptosis in Brca1-deficient mouse ovarian cancer cells. (*A*) Delivery of siParp1 confers target knockdown at the mRNA level, as determined by qPCR. BR5FVB1 cells were transfected with 5 nM siRNA, and total RNA was collected after 24 h. (*B*) Proliferation of BR5FVB1, a Brca1-deficient mouse ovarian cancer cell line that overexpresses c-myc, is inhibited by treatment with siParp1 or siMyc. Cells were transfected with 20 nM siRNA and counted 72 h after treatment. (*C*) Treatment with siParp1 causes BR5FVB1 cells to undergo apoptosis. Annexin V-PE apoptosis analysis was performed 48 h after treatment with 100 nM siRNA. Annexin V-PE positive and 7-AAD negative cells were defined as apoptotic cells by flow cytometry. NT, no treatment. siCon, siRNA targeting factor VII.

addition to performing whole-mouse imaging, we extracted the tumor nodules and visualized the fluorescently labeled siRNA, confirming the efficacy of NC100 as a delivery agent (Fig. 3*B*).

Delivery of siParp1 to Brca1-Deficient Ovarian Tumors Induces Apoptosis and Increases Survival. The BR5FVB1 cell line lacks Brca1 and overexpresses c-myc. Having confirmed that we had an siRNA sequence that knocked down c-myc protein ~85%

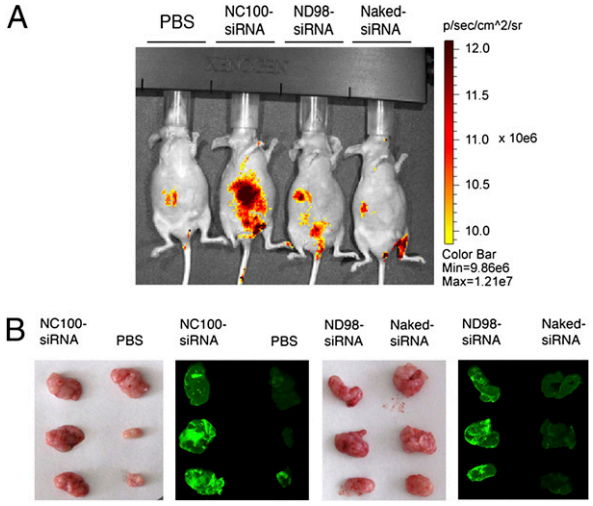

Fig. 3. Lipidoids mediate efficient siRNA delivery to murine ovarian carcinoma allograft tumors. Fluorescently labeled siRNA delivered by NC100 or ND98 is taken up by tumors in vivo following i.p. administration at a dose of 0.5 mg/kg of labeled siRNA. (*A*) Representative images of mice that were injected with PBS, Vivo-Tag 750-labeled siRNA delivered by NC100 or ND98 lipidoid nanoparticles, or naked Vivo-Tag 750-labeled siRNA. Images were taken 24 h after injection. (*B*) Detection of fluorescently labeled siRNA in the tumor nodules themselves.

(Fig. S3), we thought that siMyc would enhance the likelihood of observing a reduction in tumor growth when combined with siParp1. Indeed, our in vitro data demonstrated that BR5FVB1 cells treated with siMyc experienced a proliferation defect (Fig. 2*B*). Accordingly, mice bearing BR5FVB1-derived tumors were treated i.p. with siControl (siCon; siRNA targeting firefly luciferase for in vivo studies) or a combination of siParp1 + siMyc at a total dose of 5 mg/kg for three doses. Five animals in each group were challenged with BR5FVB1 tumor cells and, after establishment of disseminated nodules, formulated siRNAs were injected on days 14, 17, and 20. The mice were subsequently monitored, and the development of ascites in the peritoneal cavity was used as a measure of disease burden. When fluid accumulation became severe, the mice were killed. Treatment with siParp1 + siMyc reduced ascites formation and significantly ($P < 0.05$) extended survival relative to siCon (Fig. 4*A*). To test if the observed phenotype was caused by apoptotic induction, as observed in vitro by FACS analysis, TUNEL staining was performed on tumor tissue that was extracted from the mice at the time of euthanization. The number of apoptotic cells in the treated tumors was more than twice that observed in the control-treated tumors (Fig. S4).

To elucidate the contribution of c-myc oncogene knockdown relative to Parp1 knockdown, a follow-up study was performed in which siMyc and siParp1 were administered i.p. individually as well as in combination at a total dose of 5 mg/kg for six doses. Mice treated with siMyc had the same survival rate as those treated with either siCon or PBS. This suggests that the degree of growth inhibition observed with siMyc is not adequate to impact on tumor growth in vivo. In contrast, animals treated with either siParp1 alone or siParp1 + siMyc survived significantly longer ($P < 0.01$). The results indicated that the observed survival extension can be attributed solely to the targeting of Parp1 (Fig. 4*B*). Importantly, the survival effect is specific to the Brca1-deficient genotype, as it was not observed in tumors derived from Brca1 wild-type T22H cells (Fig. 4*C*), supporting the proposed mechanism of synthetic lethality. Though T22H cells experience a proliferation defect in vitro upon knockdown of c-myc, the inhibition of Parp1 does not affect their growth or induce apoptosis (Fig. S5), and the in vivo results are consistent with these observations. Immunoblotting of lysates from tumors derived from Brca1-deficient cells treated with siParp1 confirmed target knockdown in vivo (Fig. 4*D*). Notably, a lower band denoting Parp1 cleavage, a signature of apoptosis (23), was observed after two doses in the siParp1 treatment group. An examination of the Parp1 levels after a single dose of siCon vs. siParp1 confirms a greater than twofold knockdown of Parp1 by the latter. This comparison suggests that the decrease in the upper band of intact Parp1 after two doses is due not only to apoptosis-related cleavage but also to RNAi-mediated targeting of the protein.

Immunostimulation Is Not Responsible for the Observed Effect. It has been reported that some effects attributed to RNAi may actually be caused by an innate immune response to foreign nucleic acids (24). To address this possibility, we examined the immunostimulatory potential of siParp1, siMyc, and the control siRNA that were used for the in vivo experiments described previously. Whole blood was collected from mice, and a marked induction of IFN-α in serum was detected by ELISA after 6 h upon administration of NC100-formulated siParp1 compared with PBS solution or siCon; siMyc induced a moderate response (Fig. 5*A*). This response is not unusual, as it has been observed by other groups at this time-point (20). The strong immunostimulatory activity evoked by siParp1 diminished to basal level over 24 h, suggestive of a transient innate immune recognition mechanism. Still, we wanted to confirm that the observed survival extension was not due to an innate immune response.

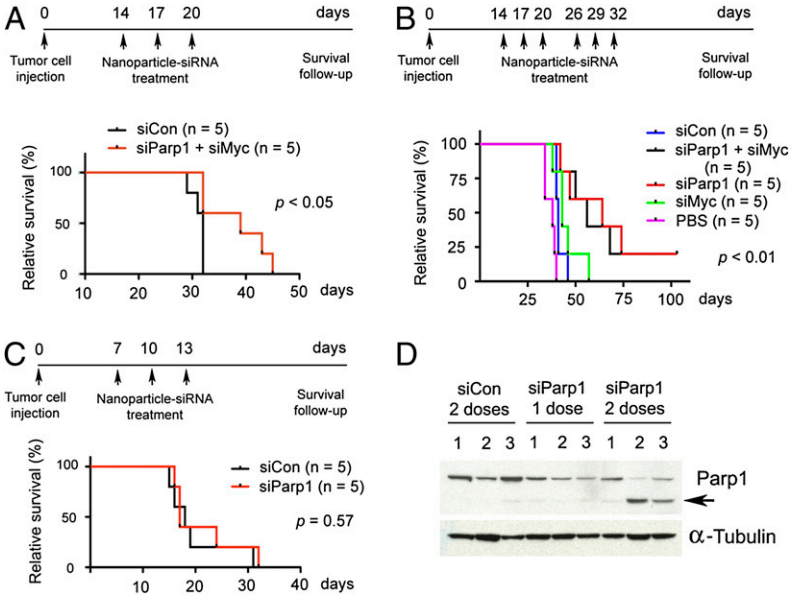

Fig. 4. Parp1 knockdown in the context of Brca1 deficiency is responsible for extension of survival. (*A*) A Kaplan–Meier curve reveals that i.p. treatment with NC100-formulated siParp1 + siMyc extends the survival of immunocompetent mice bearing tumors derived from a Brca1-deficient cell line. (*B*) The increased survival can be specifically attributed to Parp1 knockdown and not to c-myc knockdown. A Kaplan–Meier curve reveals increased survival among siParp1-treated mice when tumors are derived from a Brca1-deficient cell line. (*C*) A Kaplan–Meier curve reveals no survival difference between treatment groups when tumors are derived from a Brca1 wild-type cell line, supporting the mechanism of synthetic lethality. (*D*) Parp1 knockdown is confirmed by immunoblotting of lysates derived from extracted tumors. The arrow signifies the Parp1 cleavage product that is a hallmark of apoptosis. siCon, siRNA targeting luciferase. siRNA was administered at a dose of 5 mg/kg according to the dosing schedules shown.

Importantly, 2′-OMe-modified siParp1 (designated siParp1* herein) was nonimmunstimulatory (Fig. 5*A*), enabling us to investigate the specific causality of the knockdown of Parp1 on survival. BR5FVB1 cells were transfected with 5 nM modified or unmodified siRNA, and total RNA was collected after 48 h. Both siParp1 and siParp1* were shown to impart robust silencing, as determined by qPCR (Fig. 5*B*). After confirming that the modifications did not affect the siRNA's ability to impart mRNA knockdown, the therapeutic efficacy of siParp1* was examined by repeating the in vivo survival challenge experiment. Again, a significant survival extension was observed in the siParp1* treatment group ($P < 0.05$) compared with the control siRNA treatment group (Fig. 5*C*), suggesting that the observed immunostimulatory activity evoked by unmodified siParp1 6 h postinjection was not critical to the enhanced observed survival and that knockdown of the target gene in the context of Brca1 deficiency confers synthetic lethality.

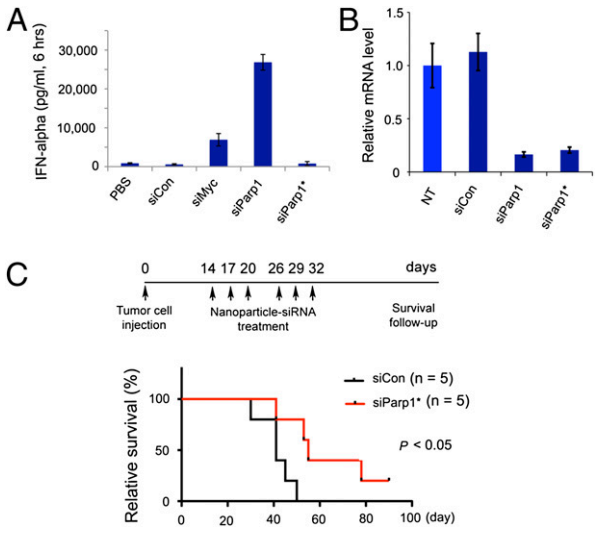

Fig. 5. The observed synthetic lethality is not attributable to immunostimulation. ELISA reveals a marked immunostimulatory response to unmodified siParp1 but not to 2′-OMe-modified siRNA (siParp1*). (*A*) IFN-α levels are shown 6 h after administration of the NC100-siRNA nanoparticle formulation. (*B*) siParp1* imparts equivalent knockdown of Parp1 mRNA as siParp, as determined by qPCR. BR5FVB1 cells were transfected with 5 nM siRNA complexed with Lipofectamine 2000, and total RNA was collected after 48 h. (*C*) siParp1* confers similar treatment efficacy to the unmodified siRNA, illustrated by significantly extended animal survival compared with control siRNA in a Brca1-deficient murine ovarian cancer model. siCon, siRNA targeting luciferase. siRNA was administered at a dose of 5 mg/kg according to the dosing schedules shown.

Discussion

We have shown that siRNA targeted against Parp1 confers synthetic lethality in vivo, extending the survival of mice bearing tumors derived from Brca1-deficient cells. These data agree with the effects observed in Brca1-deficient cells when Parp1 is drugged by a small molecule (12). Here, we show that the response is retained in a murine model of ovarian cancer. The model involves i.p. administration of materials to disseminated ovarian carcinoma allograft tumors. Delivery of lipidoid-formulated nanoparticles containing siRNA to these tumors was shown to be effective and consistent with results for a similar ovarian tumor model using a related lipidoid with siRNA targeting claudin-3 (20). These studies suggest that nanoparticle delivery to tumor cells in the i.p. cavity can be effective in the treatment of ovarian cancer. This local delivery avoids the uptake of systemically delivered nanoparticles by the liver that makes targeting to other organs difficult. In fact, there have been few reports of systemic siRNA administration to organs other than the liver (17).

Through three separate experiments in vivo, we confirm that the mechanism of action is synthetic lethality. siParp1 was administered in combination with siMyc or alone. It was administered as an unmodified or a chemically modified siRNA. The results consistently demonstrated that treatment with siParp affords extension of survival. This effect was shown to be specific to a Brca1-deficient genetic background, as the enhanced survival was not observed in a Brca1 wild-type background. The knockdown of target protein in recovered tumors was confirmed by immunoblotting. Protein cleavage, FACS analysis, and TUNEL staining indicate that the effect is primarily due to the induction of apoptosis.

The observed biology can be attributed to the knockdown of Parp1. We confirm that a second sequence against the same target similarly inhibits proliferation. Because there are 17 members of the PARP family (25), the inherent complementarity of RNA

affords another type of specificity beyond small molecules for therapeutically targeting PARP1 in the context of impaired homologous recombination. The sequence used herein, siParp1, specifically targets Parp1 but not any of the other 16 isoforms. siParp1-1 similarly targets a unique sequence in the distinctive 5′ end of the target mRNA transcript. This is important because Parp2 is the only other PARP family member that has been implicated in DNA repair, and the functions of the other isoforms are very important to the cell, including cell cycle control (PARP-3), intracellular transport (PARP-4), regulation of telomere length (PARP-5a) and chromatin structure (PARP-10), and antiviral responses (PARP-13) (25).

The inhibition of PARP1 might also be used to address sporadic cancers that exhibit "BRCAness," the functional traits of *BRCA* mutation in the absence of actual mutations (26). Though not detected in normal tissue, aberrant methylation of the *BRCA1* promoter and silencing of expression are found in 11–14% of breast cancers and 5–31% of ovarian cancers (6, 27). This epigenetic pattern is typically restricted to these two cancers, consistent with the tumorigenicity of *BRCA* mutations. Notably, promoter methylation of Fanconi anemia complementation group F (*FANCF*), which inactivates the FANC-BRCA pathway, has been observed in several other types of sporadic cancer (28, 29). In addition to epigenetic alterations at the genomic level, functional inactivation of BRCA at the protein level is also possible (30). EMSY, which has been reported to bind to the activation domain of BRCA2, thereby inhibiting its activity, is amplified in sporadic breast cancer (13%) and higher-grade ovarian cancer (17%) (26). Thus, the range of cancers that might specifically respond to siParp1 could be much larger than just those with mutations in BRCA genes.

Our findings validate the possibility of assaying ovarian cancer in its native context, the i.p. setting of immunocompetent animals, for the effect of inhibition of specific genes on tumorigenesis. For example, nanoparticle-mediated delivery of siRNA targeting ErbB3 (31) could be used to investigate the dependence of ovarian cancer on downstream signaling pathways. Here, we show that nanoparticle-mediated i.p. delivery of siRNA targeting Parp1 to disseminated tumors, which resemble the presentation in humans, can induce apoptosis and extend survival specifically in a Brca1-deficient genetic background. These findings raise the possibility of creating synthetic lethal phenotypes through the delivery of siRNA combinations, because multiple siRNAs can be delivered simultaneously in nanoparticles (19).

Materials and Methods

Cell Lines and Mouse Models. We have previously generated genetically defined murine ovarian cancer cell lines based on an RCAS-TVA gene delivery system (21, 22). To establish mT2K cells, T2 cells (p53$^{-/-}$, Akt, myc) were infected in vitro with RCAS-K-ras^{G12D} virus. To establish T22H cells, T22 cells (an independently derived cell line with p53$^{-/-}$, Akt, myc background) were infected in vitro with pBabe-puro-H-ras^{V12} and subsequently selected for 10 d in media containing 2.0 μg/mL of puromycin. T22H cells were able to grow in both immunodeficient nude mice and immunocompetent FVB mice. Tumor nodules from immunocompetent FVB mice injected with the Brca1-deficicient cell line BR5 were used to generate the BR5FVB1 tumor cell line, which was able to grow in recipient FVB mice. The stably luciferase-expressing cell lines mT2K-Luc and BR5FVB1-Luc were generated by infecting mT2K cells and BR5FVB1 cells with pMSCV-puro-Firefly luciferase viral supernatant and selecting the cells in a medium containing 2.0 μg/mL of puromycin. To generate allografts, 1×10^6 murine ovarian cancer cells in 150 μL of Opti-MEM media (Invitrogen) were injected i.p. into 5- to 6-wk-old female athymic nude mice or female FVB/NJ mice (Jackson Laboratory). Tumors and/or visible ascites generally developed within 4–7 wk of injection, depending on the distinct genetic composition of the cell lines. All studies on mice were approved by the Massachusetts Institute of Technology Committee on Animal Care.

siRNAs. siRNAs targeting luciferase (siLuc), GFP (siGFP), or factor VII (siFVII) and 2′-OMe-modified siRNA targeting murine Parp1 (siParp1*) were synthesized by Alnylam Pharmaceuticals. Unmodified siRNAs targeting murine Parp1 (siParp1 and siParp1-1) or human Myc (siMyc) were synthesized by and purchased from Dharmacon. The sequences for the sense and antisense strands of siRNAs are as follows:

siLuc sense: 5′- AACGCUGGGCGUUAAUCAAdTdT-3′; antisense: 5′-UUGAUUAACGCCCAGCGUUdTdT-3′.
siGFP sense: 5′-CCACAUGAAGCAGCACGACdTdT-3′; antisense: 5′-GUCGUGCUGCUUCAUGUGGdTdT-3′.
siFVII sense: 5′-GGAUCAUCUCAAGUCUUACdTdT-3′; antisense: 5′-GUAAGACUUGAGAUGAUCCdTdT-3′.
siParp1 sense: 5′-CCAAAGGAAUUCCGAGAAAdTdT-3′; antisense: 5′-UUUCUCGGAAUUCCUUUGGdTdT-3′.
siParp1-1 sense: 5′-CCAUCAAGAAUGAAGGAAAdTdT-3′; antisense: 5′-UUUCCUUCAUUCUUGAUGGdTdT-3′.
siMyc sense: 5′-GGACUAUCCUGCUGCCAAGdTdT-3′; antisense: 5′-CUUGGCAGCAGGAUAGUCCdTdT-3′.

The sequence of the modified Parp1 siRNA (siParp1*) is as follows:

sense: 5′-ccAAAGGAAuuccGAGAAAdTdT-3′; antisense: 5′-UUUCUcGGAAUUCCuuGGdTdT-3′.
A, C, G, U are ribonucleotides; dT is deoxythymidine; and c and u are 2′-OMe-modified pyrimidines.

Lipidoid Synthesis. Lipidoids were synthesized and purified as described previously (19).

Lipidoid Screening. A total of 8,000 cells/well of mT2K-Luc cells were plated into 96-well plates in DMEM with 10% FCS and 1% penicillin/streptomycin. After 2 d of growth in culture, the cells were transfected with lipidoid-siRNA complexes. Briefly, individual lipidoids were premixed with siLuc or siGFP at a weight-to-weight ratio of 2.5:1 (optimized transfection conditions were determined empirically). The working concentration of siRNAs used for screening was 10 nM. Working solutions of each lipidoid were prepared in 25 mM sodium acetate buffer (pH 5.2). The transfection mixtures were incubated for 20 min to allow for complex formation, and 30 μL of each of the lipidoid/siRNA solutions was then added to 200 μL of medium in 96-well plates. Cells were allowed to grow at 37 °C with 5% CO_2 and lysed 24 h after transfection. Firefly luciferase activity was determined using the Luciferase Assay Kit (Promega) according to the manufacturer's instructions. Lipofectamine 2000 (Invitrogen) was used as a positive transfection control. Transfections were performed in triplicate.

Cell Proliferation Assay. To monitor cell proliferation, cells transfected with 20 nM siCon (siRNA targeting factor VII) or siParp1 were harvested 72 h after transfection, and cell proliferation was determined by measuring luciferase activity as described previously (32). The lipidoid-siRNA transfection protocol is described above.

In Vitro Apoptosis Assay. Brca1-deficient BR5FVB1 cells were transfected with 100 nM siCon (siRNA targeting factor VII) or siParp1 complexed with NC100. At 48 h after transfection, cells were washed and resuspended at a concentration of 1×10^6 cells/mL. The apoptotic cells were determined by flow cytometry using Annexin V-PE Apoptosis Detection Kit I according to the manufacturer's instructions (BD Biosciences). Cells with positive Annexin V-PE and negative 7-AAD represented early apoptotic cells. The experiments were performed in triplicate.

Lipidoid-siRNA Nanoparticle Formulation and Treatment in Vivo. siRNAs targeting Parp1 or Luciferase were formulated with NC100 lipidoid, PEG ceramide, and cholesterol as described previously for ND98 (19). The formulated lipidoid-siRNA nanoparticles were determined to be ~75 nm by dynamic light scattering using a Zetasizer Nano ZS (Malvern). To assess in vivo efficacy, female nude or FVB mice were injected i.p. with 1×10^6 cells in Opti-MEM media. For the Brca1 wild-type cell line T22H, 7 d after the initial injection of cells, the mice were treated with 250 μL of NC100-siRNA nanoparticle solution (5 mg/kg i.p.) every 3 d for three doses. For the Brca1-deficient cell line BR5FVB1, 14 d after the initial injection of cancer cells, mice were treated with 250 μL of nanoparticle solution (5 mg/kg i.p.) every 3 d for three doses, skipping one dose to mimic cyclic chemotherapeutic dosing, and then an additional three doses every 3 d. Mice were euthanized if they exhibited visible tumors or significant ascites. Mean survival time was calculated using the Log-rank test. Kaplan–Meier survival curves were drawn using GraphPad PRISM software. For the lipidoid-siRNA nanoparticle tolerance assay, mice were injected with PBS, sodium acetate, and escalating

doses of NC100-siRNA nanoparticles (2.5, 5, 7.5, and 10 mg/kg of siRNA). The body weights of mice were measured before injection and on postinjection days 1 and 3.

Synthesis of Fluorescently Labeled siRNA. siRNA against firefly luciferase (sense: CUUACGCUGAGUACUUCGA; antisense: UCGAAGUACUCAGCGUAAG) was obtained from Dharmacon. The 5′ end of the sense strand was modified with a 5′-amino, six-carbon linker. Near-infrared fluorophore-labeled siRNA was prepared by mixing the unlabeled siRNA duplex with a 100-fold molar excess of VivoTag-750-NHS-ester (Visen Medical) in PBS. The mixture was stirred at room temperature for 2 h. The fluorophore-siRNA conjugate was separated from excess fluorophore by ethanol precipitation and resuspended in RNase-free water.

In Vivo Imaging. Brca1 wild-type T22H mouse ovarian cancer cells were injected i.p. into nude mice and allowed to grow for 14 d. The mice were then injected i.p. with PBS, naked fluorophore-labeled siRNA, or fluorophore-labeled siRNA formulated with NC100 or ND98 nanoparticles. Fluorochrome absorption was visualized using an IVIS Spectrum bioluminescent and fluorescent imaging system (Caliper Life Sciences).

Quantitative PCR. Total RNA was extracted from tumors using TRIzol reagent (Invitrogen) according to the manufacturer's instructions. One microgram of total RNA was used for reverse transcription using the ImProm-II Reverse Transcription System Kit (Promega). The quantitative PCR was performed using SYBR Green PCR Master Mix reagent (Applied Biosystems). The average threshold cycle for each gene was determined from triplicate reactions, and the expression level was normalized to GAPDH. The primers used for detecting the expression levels of murine Parp1 and GAPDH were as follows: Parp1-F: 5′-CCA TCG ACG TCA ACT ACG AG-3′, Parp1-R: 5′-GTG CGT GGT AGC ATG AGT GT-3′. GAPDH-F: 5′-CAT GGC CTT CCG TGT TCC TA, GAPDH-R: 5′-CCT GCT TCA CCA CCT TCT TGA T-3′.

Western Blotting. Frozen tumor tissues from mice injected with Brca1-deficient BR5FVB1 cells and treated with either siLuc or siParp1 were minced and homogenized in cold modified RIPA buffer (Sigma) with a protease inhibitor mix (Roche). Equal amounts of total protein lysate were denatured in Laemmeli buffer at 70 °C for 5 min, separated by a 4–12% SDS/PAGE NuPage gel (Invitrogen) and transferred to PVDF membranes. Anti-murine Parp1 (Cell Signaling) was used at a 1:1,000 dilution in 5% milk. Anti-human c-myc (Santa Cruz Biotechnologies) was used at a 1:500 dilution in 5% milk. Anti-α-tubulin (Sigma) was used as a loading control at a 1:10,000 dilution in 5% milk. The proteins were detected using an ECL detection system (Perkin-Elmer) according to the manufacturer's instructions.

TUNEL Staining. Fresh tumor tissues from mice injected with Brca1-deficient BR5FVB1 cells and treated with either siLuc or siParp1 were biopsied, immediately snap frozen, embedded in Optimal Cutting Temperature (OCT) reagent (Sakura Finetek), and stored at −80 °C. Frozen tissue sections (5 μm) were cut with a cryostat and fixed with 4% paraformaldehyde in PBS (pH 7.4). The apoptotic cells were detected using the In Situ Cell Death Detection Kit, TMR red, according to the manufacturer's instructions (Roche).

Cytokine ELISA. Six and 24 h following i.p. injection of NC100-formulated siRNA (5 mg/kg), blood serum was collected and used for ELISA of mouse IFN-α using the Verikine Mouse Interferon Alpha (Mu-IFN-α) ELISA Kit according to the manufacturer's instructions (PBL Biomedical).

Statistical Analysis. Statistical analysis was carried out using a two-tailed Student's *t* test. A value of $P < 0.05$ was considered to be statistically significant.

ACKNOWLEDGMENTS. We thank E. Vasile for assistance with microscopy; D. Crowley and A. Caron for assistance with histology; G. Paradis for assistance with FACS analysis; and D. Anderson for critical reading of the manuscript. This work was supported by MIT-Harvard Center for Cancer Nanotechnology Excellence Grant U54 CA119349 from the National Cancer Institute, the Marie D. and Pierre Casimir-Lambert Fund, and partially by the Cancer Center Support (core) Grant P30-CA14051 from the National Cancer Institute. siRNAs for animal experiments were generously provided by Alnylam Pharmaceuticals, Inc.

1. Bast RC, Jr., Hennessy B, Mills GB (2009) The biology of ovarian cancer: New opportunities for translation. *Nat Rev Cancer* 9:415–428.
2. Yap TA, Carden CP, Kaye SB (2009) Beyond chemotherapy: Targeted therapies in ovarian cancer. *Nat Rev Cancer* 9:167–181.
3. Easton DF, Ford D, Bishop DT; Breast Cancer Linkage Consortium (1995) Breast and ovarian cancer incidence in BRCA1-mutation carriers. *Am J Hum Genet* 56:265–271.
4. Stratton JF, et al. (1997) Contribution of BRCA1 mutations to ovarian cancer. *N Engl J Med* 336:1125–1130.
5. Rubin SC, et al. (1998) BRCA1, BRCA2, and hereditary nonpolyposis colorectal cancer gene mutations in an unselected ovarian cancer population: Relationship to family history and implications for genetic testing. *Am J Obstet Gynecol* 178:670–677.
6. Catteau A, Harris WH, Xu CF, Solomon E (1999) Methylation of the BRCA1 promoter region in sporadic breast and ovarian cancer: Correlation with disease characteristics. *Oncogene* 18:1957–1965.
7. Annunziata CM, O'Shaughnessy J (2010) Poly (adp-ribose) polymerase as a novel therapeutic target in cancer. *Clin Cancer Res* 16:4517–4526.
8. Venkitaraman AR (2002) Cancer susceptibility and the functions of BRCA1 and BRCA2. *Cell* 108:171–182.
9. Moynahan ME, Chiu JW, Koller BH, Jasin M (1999) Brca1 controls homology-directed DNA repair. *Mol Cell* 4:511–518.
10. Krishnakumar R, Kraus WL (2010) The PARP side of the nucleus: Molecular actions, physiological outcomes, and clinical targets. *Mol Cell* 39:8–24.
11. Dantzer F, et al. (2000) Base excision repair is impaired in mammalian cells lacking Poly(ADP-ribose) polymerase-1. *Biochemistry* 39:7559–7569.
12. Farmer H, et al. (2005) Targeting the DNA repair defect in BRCA mutant cells as a therapeutic strategy. *Nature* 434:917–921.
13. Bryant HE, et al. (2005) Specific killing of BRCA2-deficient tumours with inhibitors of poly(ADP-ribose) polymerase. *Nature* 434:913–917.
14. Fong PC, et al. (2009) Inhibition of poly(ADP-ribose) polymerase in tumors from BRCA mutation carriers. *N Engl J Med* 361:123–134.
15. Ashworth A (2008) A synthetic lethal therapeutic approach: Poly(ADP) ribose polymerase inhibitors for the treatment of cancers deficient in DNA double-strand break repair. *J Clin Oncol* 26:3785–3790.
16. Bumcrot D, Manoharan M, Koteliansky V, Sah DW (2006) RNAi therapeutics: A potential new class of pharmaceutical drugs. *Nat Chem Biol* 2:711–719.
17. Davis ME, et al. (2010) Evidence of RNAi in humans from systemically administered siRNA via targeted nanoparticles. *Nature* 464:1067–1070.
18. Armstrong DK, et al.; Gynecologic Oncology Group (2006) Intraperitoneal cisplatin and paclitaxel in ovarian cancer. *N Engl J Med* 354:34–43.
19. Akinc A, et al. (2008) A combinatorial library of lipid-like materials for delivery of RNAi therapeutics. *Nat Biotechnol* 26:561–569.
20. Huang YH, et al. (2009) Claudin-3 gene silencing with siRNA suppresses ovarian tumor growth and metastasis. *Proc Natl Acad Sci USA* 106:3426–3430.
21. Xing D, Orsulic S (2005) A genetically defined mouse ovarian carcinoma model for the molecular characterization of pathway-targeted therapy and tumor resistance. *Proc Natl Acad Sci USA* 102:6936–6941.
22. Xing D, Orsulic S (2006) A mouse model for the molecular characterization of brca1-associated ovarian carcinoma. *Cancer Res* 66:8949–8953.
23. Pastorino JG, Chen ST, Tafani M, Snyder JW, Farber JL (1998) The overexpression of Bax produces cell death upon induction of the mitochondrial permeability transition. *J Biol Chem* 273:7770–7775.
24. Kleinman ME, et al. (2008) Sequence- and target-independent angiogenesis suppression by siRNA via TLR3. *Nature* 452:591–597.
25. Schreiber V, Dantzer F, Ame JC, de Murcia G (2006) Poly(ADP-ribose): Novel functions for an old molecule. *Nat Rev Mol Cell Biol* 7:517–528.
26. Turner N, Tutt A, Ashworth A (2004) Hallmarks of 'BRCAness' in sporadic cancers. *Nat Rev Cancer* 4:814–819.
27. Esteller M, et al. (2000) Promoter hypermethylation and BRCA1 inactivation in sporadic breast and ovarian tumors. *J Natl Cancer Inst* 92:564–569.
28. Marsit CJ, et al. (2004) Inactivation of the Fanconi anemia/BRCA pathway in lung and oral cancers: Implications for treatment and survival. *Oncogene* 23:1000–1004.
29. Narayan G, et al. (2004) Promoter hypermethylation of FANCF: Disruption of Fanconi Anemia-BRCA pathway in cervical cancer. *Cancer Res* 64:2994–2997.
30. Hughes-Davies L, et al. (2003) EMSY links the BRCA2 pathway to sporadic breast and ovarian cancer. *Cell* 115:523–535.
31. Sheng Q, et al. (2010) An activated ErbB3/NRG1 autocrine loop supports in vivo proliferation in ovarian cancer cells. *Cancer Cell* 17:298–310.
32. Coombe DR, Nakhoul AM, Stevenson SM, Peroni SE, Sanderson CJ (1998) Expressed luciferase viability assay (ELVA) for the measurement of cell growth and viability. *J Immunol Methods* 215:145–150.

Supporting Information

Goldberg et al. 10.1073/pnas.1016538108

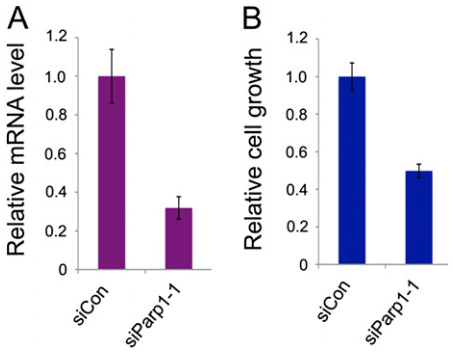

Fig. S1. Induction of the observed phenotype is not limited to a single siRNA sequence targeting Parp1. A reduction in proliferation is observed when Brca1-deficient cells are treated with NC100-formulated siRNA that targets a distinct sequence within the target gene. (*A*) Delivery of siParp1-1 confers target knockdown at the mRNA level, as determined by qPCR. BR5FVB1 cells were transfected with 5 nM siRNA, and total RNA was collected after 48 h. (*B*) Proliferation of BR5FVB1, a Brca1-deficient mouse ovarian cancer cell line, is inhibited by treatment with siParp1-1. Cells were transfected with 20 nM siRNA and counted 72 h after treatment. siCon, siRNA targeting factor VII.

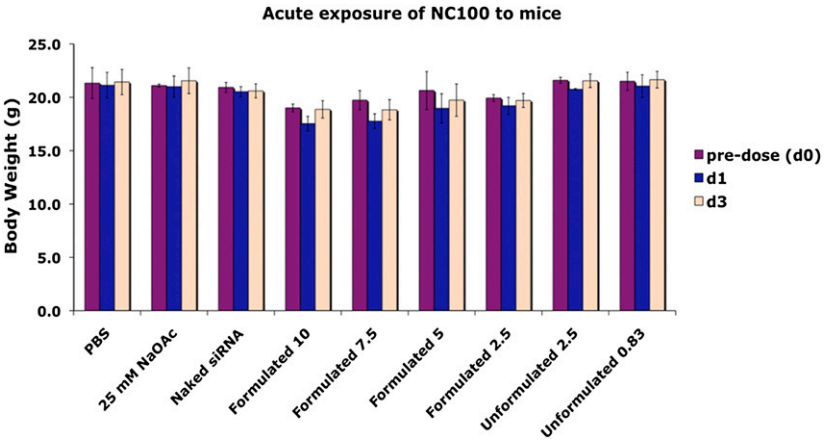

Fig. S2. The safety of NC100 was confirmed by delivering escalating doses of lipidoid-siRNA nanoparticles and monitoring body weight as a proxy for tolerability. NC100 was well tolerated at all doses (mg/kg siRNA indicated on *x* axis), with a minor decrease observed after 24 h that was readily restored by 72 h postinjection. Though more substantial at the higher doses, the decrease in weight is not statistically significant at the dose used in the survival studies (5 mg/kg). "Unformulated" refers to a crude mixture of lipidoid and siRNA. Formulated refers to the addition of cholesterol and PEG-ceramide as excipients followed by extrusion to attain monodisperse particle size (*Materials and Methods*).

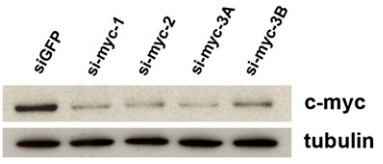

Fig. S3. siRNA targeting c-myc effectively knocks down protein expression. Cells were transfected with 20 nM siRNA using several sequences that target the c-myc transcript. Lysates were collected after 48 h, and immunoblotting confirmed that si-myc-3A was the most potent sequence, so this sequence was used for the subsequent in vitro and in vivo studies. siRNA targeting GFP was used as a negative control.

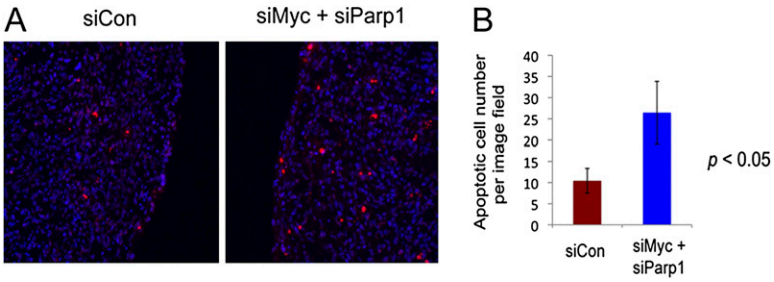

Fig. S4. Treatment with siMyc + siParp1 results in the induction of apoptosis in vivo. (*A*) TUNEL staining of extracted Brca1-deficient tumors. (*B*) Quantification of the images confirms a statistically significant increase in the number of apoptotic cells in treated tumors.

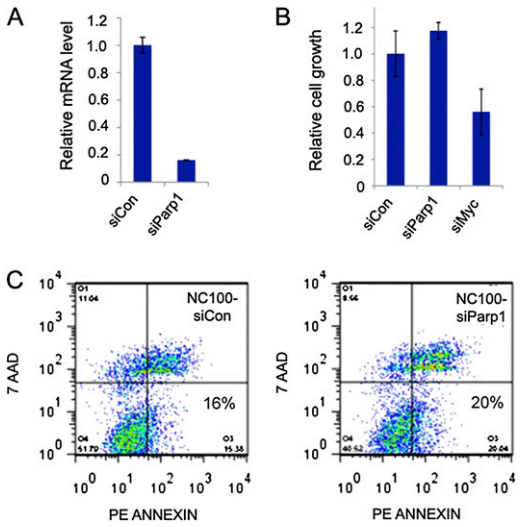

Fig. S5. Brca1 wild-type ovarian cancer cells are unaffected by the knockdown of Parp1 in vitro. (*A*) siParp1 confers target knockdown at the mRNA level, as determined by qPCR. T22H cells were transfected with 5 nM siRNA, and total RNA was collected after 24 h. (*B*) Proliferation of T22H is inhibited by treatment with siMyc but not by treatment with siParp1. Cells were transfected with 20 nM siRNA and counted 72 h after treatment. (*C*) Treatment with siParp1 does not cause T22H cells to undergo increased apoptosis. Annexin VPE apoptosis analysis was performed 48 h after treatment with 100 nM siRNA. Annexin V-PE positive and 7-AAD negative cells were defined as apoptotic cells by flow cytometry. siCon, siRNA targeting factor VII.